RESEARCH PAPERS

Acta Cryst. (1997). B53, 7–17

Structure of $Na_3NdSi_6O_{15}.2H_2O$ – a Layered Silicate with Paths for Possible Fast-Ion Conduction

S. M. HAILE,[a]* B. J. WUENSCH,[b] R. A. LAUDISE[c] AND J. MAIER[d]

[a]*Department of Materials Science and Engineering, University of Washington, Seattle, WA 98195–2120, USA,* [b]*Department of Materials Science and Engineering, Massachusetts Institute of Technology, Cambridge, MA 02139-4307, USA,* [c]*Lucent Technologies, Bell Laboratories, Murray Hill, NJ 07974-0636, USA, and* [d]*Max-Planck-Institut für Festkörperforschung D-70569 Stuttgart, Germany. E-mail: smhaile@u.washington.edu*

(*Received 7 May 1996; accepted 24 July 1996*)

Abstract

Hydrothermal investigations of the high silica region of the Na_2O–Nd_2O_3–SiO_2 system, carried out in the search for new fast-ion conductors (FIC's), yielded the compound $Na_3NdSi_6O_{15}.2H_2O$ (sodium neodymium silicate). Single-crystal X-ray methods provided lattice constants of $a = 7.385\,(2)$, $b = 30.831\,(7)$ and $c = 7.1168\,(13)$ Å, space group *Cmm*2, and 22 atoms in the asymmetric unit. With four formula units per unit cell, the calculated density is $2.68\ g\ cm^{-3}$. Refinement was carried out with 1113 independent structure factors to a weighted residual $wR(F)$ of 2.63% [8.09% for $wR(F^2)$] using anisotropic temperature factors for all atoms. The structure, based on corrugated Si_6O_{15} layers containing four-, five-, six- and eight-membered rings, is related to that of a model previously reported for a compound assigned the composition $NaNdSi_6O_{13}(OH)_2.nH_2O$. Our structure differs in the placement of sodium ions and water molecules, and contains no hydroxyl groups. We believe that both studies examined the same phase.

1. Introduction

Ever since Goodenough, Hong & Kafalas (1976) reported high sodium-ion mobility in NASICON, $Na_{1+x}Zr_2P_{3-x}Si_xO_{12}$, alkali silicates have been the subject of continued investigations of their ion transport properties. We were especially interested in preparing and characterizing the compound $Na_3NdSi_6O_{15}$ as we had previously measured the conductivity of $K_3NdSi_6O_{15}$ (Haile, Wuensch, Siegrist & Laudise, 1992) and found it to have a reasonably high conductivity for a material in which K^+ is the mobile species. We expected that the sodium analog, having a smaller and typically more mobile species as the charge carrier, might exhibit fast-ion conduction. Furthermore, the anisotropy we had observed in the conductivity of $K_3NdSi_6O_{15}$ and $K_3NdSi_3O_8(OH)_2$ [Hale (*sic*), Maier, Wuensch & Laudise, 1993] suggested that this family of compounds constitutes an ideal set of model materials for correlating structural features to observed conductivities.

2. Experimental

2.1. *Crystal growth*

The crystal growth of compounds with high silica content is hindered by the tendency of these materials to form stable glasses. The hydrothermal method, which employs high temperatures and pressures to dissolve a normally insoluble precursor material and precipitate the stable crystalline phase, has been utilized because of its effectiveness in aiding crystallization in such glass-forming systems (Laudise, 1987). Crystals of $Na_3NdSi_6O_{15}.2H_2O$, approximately 50 μm in size, were obtained as a single-phase product in a synthesis of 10 d duration at the temperature 673 K (isothermal) and pressure 8.25×10^5 Pa. The precursor, a powdered glass of composition $4Na_2O$–Nd_2O_3–$17SiO_2$, was placed in a solvent of 0.1 *M* NaOH. Further details of this synthesis and the range of conditions under which the phase was formed are described elsewhere (Haile, 1992; Haile, Wuensch & Laudise, 1993).

2.2. *Composition determination*

The compositions of crystals thus obtained were determined from electron microprobe measurements. Small crystals were mounted in an epoxy resin and polished. These were then sputter-coated using a gold/palladium electrode. Data were collected with a Jeol Superprobe 733 equipped with a wavelength-dispersive detector. Characteristic peak intensities were converted to stoichiometric quantities using the *ZAF* data reduction program (Schamber, Wodke & McCarthy, 1981). The standards employed were SiO_2 glass and a NdF_3 single crystal for Si and Nd, respectively; sodalite or amelia albite glass were used for Na. These measurements yielded mole percentages for Na, Nd and

Table 1. *The results of electron microprobe analyses at three different locations within a single crystal of the present sodium neodymium silicate*

The expected values are those calculated for the composition $Na_3NdSi_6O_{15}.2H_2O$, deduced from the chemical analysis and the structure determination.

Position	Na mol%	Nd mol%	Si mol%	Total wt% oxides
1	10.81	3.49	22.40	94.55
2	10.79	3.50	22.50	94.77
3	10.74	3.46	22.24	94.19
Average	10.78 (4)	3.48 (2)	22.4 (1)	94.5 (3)
Expected	10.5	3.5	21.0	94.7

Si of 10.78 (4), 3.48 (2) and 22.4 (1), respectively (Table 1). From this, we calculate a total weight percent of the corresponding oxides of 94.5 (3), implying a water content of 5.5 (3) wt% for a composition in which the missing weight is attributed entirely to H_2O. A composition of $Na_3NdSi_6O_{15}.2H_2O$ corresponds to ideal Na, Nd and Si mole percentages of 10.5, 3.5 and 21.0, respectively, and a water content of 5.3 wt%.

The water content was also determined from the observation of weight loss under heating in a Netzsch thermogravimetric balance (model STA). Using a heating rate of 20 K min^{-1} and with the specimen in a vacuum of ~1 Pa, the data indicated a loss of 3.8 wt%. Mass spectrometry of the exiting gas confirmed it to be entirely water vapor. The presence of two distinct H_2O peaks in the emissions spectrum (at 413 and 473 K) suggested that the water molecules are located in at least two crystallographically distinct sites.

2.3. *Structure determination*

Full details of the data collection parameters are provided in Table 2. An analysis of the systematic absences gave *mmmC**** as the diffraction symbol, permitting *Cmmm*, *Cmm*2, *Cm*2*m* and *C*222 as possible space groups. *Cmm*2 proved to be the correct choice. Structure-factor calculations and least-squares refinement were carried out using the *SHELXL*93 program (Sheldrick, 1993), in which a residual based on F^2 values is minimized, only very negative data are excluded from the refinement and a floating point origin is utilized for space groups without a defined origin (Flack, 1983). Unless otherwise indicated, all residuals refer to $wR(F^2)$. Complete details of the refinement are also given in Table 2.

The combination of lattice constants and diffraction symbol determined was very similar to data reported for the compound $NaNdSi_6O_{13}(OH)_2.nH_2O$ (space group *Cmm*2) by Karpov, Pushcharovskii, Pobedimskaya, Burshtein & Belov (1977). However, the present microprobe analysis (Table 1) indicates a composition substantially richer in Na. We proceeded to refine the structure using the coordinates of the 17 atoms in the asymmetric unit provided by Karpov, Pushcharovskii,

Table 2. *Experimental details*

Crystal data	
Chemical formula	$Na_3NdSi_6O_{15}.2H_2O$
Chemical formula weight	657.75
Cell setting	Orthorhombic
Space group	*Cmm*2
a (Å)	7.385 (2)
b (Å)	30.831 (7)
c (Å)	7.1168 (13)
V (Å^3)	1620.4 (6)
Z	4
D_x (Mg m^{-3})	2.68
Radiation type	Mo $K\alpha$
Wavelength (Å)	0.71073
No. of reflections for cell parameters	21
θ range (°)	8.6–11.7
μ (mm^{-1})	3.816
Temperature (K)	298 (3)
Crystal form	Irregular
Crystal size (mm)	0.05 × 0.04 × 0.01
Crystal color	Clear, light blue
Data collection	
Diffractometer	Philips four-circle PW1100
Data collection method	Wyckoff scans
Absorption correction	Ψ scan
T_{min}	0.063
T_{max}	0.103
No. of measured reflections	1113
No. of independent reflections	1113
No. of observed reflections	1113
Criterion for observed reflections	$I \geq -2\sigma(I)$
θ_{max} (°)	27.5
Range of h, k, l	$0 \rightarrow h \rightarrow 9$ $0 \rightarrow k \rightarrow 40$ $0 \rightarrow l \rightarrow 9$
No. of standard reflections	29
Frequency of standard reflections	Every 30 reflections
Intensity decay (%)	0.40
Refinement	
Refinement on	F^2
$R[F^2 > -2\sigma(F^2)]$	0.0805
$wR(F^2)$	0.0809
S	0.507
No. of reflections used in refinement	1113
No. of parameters used	158
H-atom treatment	H atoms not located
Weighting scheme	$w = 1/[\sigma^2(F_o^2) + 0.1227P^2 + 59.8687P]$, where $P = 1/3(F_o^2 + F_c^2)$
$(\Delta/\sigma)_{max}$	0.112
$\Delta\rho_{max}$ (e Å^{-3})	0.866
$\Delta\rho_{min}$ (e Å^{-3})	−0.863
$\Delta\rho_{mean}$ (e Å^{-3})	0.148
Extinction method	None
Source of atomic scattering factors	Cromer & Waber (1974)

Pobedimskaya, Burshtein & Belov (1977). A rather high residual, ~16%, was obtained. Also, the temperature factor for one of the O atoms became nonpositive definite. An electron-density difference map revealed the presence of significant electron density at a number of additional locations (also reported by Karpov, Pushcharovskii, Pobedimskaya, Burshtein & Belov, 1977). Na atoms and water molecules, some with partial occupancies, were introduced to five sites, leading to a reduction of the residual to approximately 8% and the elimination of nonphysical thermal parameters. The

Table 3. *Atomic coordinates of $Na_3NdSi_6O_{15}.2H_2O$*

The e.s.d.'s in the last digit(s) are given in parentheses. O_w indicates the location of a water molecule. O atoms of Karpov, Pushcharovskii, Pobedimskaya, Burshtein & Belov (1977) listed in bold typeface were considered to be 1/3 OH and 2/3 O by these authors.

	Present work				Karpo *et al.**		
	Position	*x*	*y*	*z*	*x*	*y*	*z*
Nd	(4*e*)*m*..	1/2	0.36890 (1)	0.99823 (9)	Nd 1/2	0.3690	0.9984
Na(1)	(4*e*)*m*..	0.0	0.3760 (2)	0.9743 (15)	Na 0	0.3760	0.9743
Na(2)†	(8*f*)	0.2815 (10)	0.2376 (3)	0.1388 (12)	-		
Na(3)‡	(2*a*)*mm*2	1/2	1/2	0.842 (2)	R(1)§ 1/2	1/2	0.831
Na(4)‡	(8*f*)	0.2417 (12)	0.4627 (3)	0.7888 (13)	-		
Si(1)	(4*e*)*m*..	1/2	0.41599 (7)	0.5077 (6)	Si(1) 1/2	0.4156	0.5024
Si(2)	(8*f*)	0.2080 (2)	0.29814 (6)	0.7117 (3)	Si(4) 0.2084	0.2981	0.7068
Si(3)	(4*e*)*m*..	1/2	0.31787 (9)	0.4044 (4)	Si(3) 1/2	0.3178	0.3982
Si(4)	(8*f*)	0.2093 (3)	0.45021 (7)	0.2481 (3)	Si(2) 0.2108	0.4508	0.2434
O(1)	(8*f*)	0.3222 (7)	0.3029 (2)	0.5194 (12)	O(7) 0.319	0.303	0.516
O(2)	(8*f*)	0.2601 (7)	0.4179 (2)	0.0851 (8)	**O(4)** 0.258	0.417	0.080
O(3)	(4*e*)*m*..	1/2	0.3711 (2)	0.3811 (13)	O(1) 1/2	0.371	0.384
O(4)	(4*e*)*m*..	0.0	0.2992 (2)	0.6374 (12)	O(9) 0.0	0.298	0.629
O(5)	(4*c*)..2	1/4	1/4	0.7998 (13)	O(8) 1/4	1/4	0.805
O(6)	(4*e*)*m*..	1/2	0.3005 (2)	0.1943 (12)	**O(11)** 1/2	0.301	0.187
O(7)	(4*e*)*m*..	0.0	0.5456 (3)	0.3124 (12)	O(5) 0.0	0.446	0.302
O(8)	(8*f*)	0.3218 (7)	0.5428 (2)	0.4425 (8)	O(2) 0.324	0.442	0.439
O(9)	(8*f*)	0.2500 (7)	0.3330 (2)	0.8680 (9)	**O(6)** 0.250	0.333	0.867
O(10)	(4*e*)*m*..	1/2	0.4099 (2)	0.7281 (10)	**O(10)** 1/2	0.410	0.718
O(11)	(4*d*).*m*.	0.2426 (11)	1/2	0.1785 (12)	O(3) 0.238	1/2	0.175
$O_w(1)$	(4*e*)*m*..	0.0	0.3097 (4)	0.206 (2)	R(3)§ 0.0	0.306	0.192
$O_w(2)$†	(8*f*)	0.076 (2)	0.4471 (6)	0.769 (2)	R(2)§ 0.0	0.451	0.666

* No standard deviations for atomic coordinates were provided. † Fixed occupancy of 1/2, atom split over two neighboring sites. ‡ Refined occupancies: Na(3) = 0.55 (2), Na(4) = 0.365 (7). Sum fixed such that K[Na(3)] + 4 K[Na(4)] = 2. § Location of residual electron density in final difference Fourier map.

Table 4. *Thermal parameters of $Na_3NdSi_6O_{15}.H_2O$*

The e.s.d's in the last digit(s) are given in parentheses. Anisotropic temperature factors are of the form $\exp[-2\pi^2(h^2U^{11}a^{*2} + \ldots + hkU^{12}a^*b^* + \ldots)]$ and are given in units of 10^{-2} Å^2. U_{iso} is defined as $(1/3)\Sigma_i\Sigma_j U^{ij}a_i^*a_j^*\mathbf{a}_i.\mathbf{a}_j$.

	U_{iso}	U^{11}	U^{22}	U^{33}	U^{23}	U^{13}	U^{12}
Nd	1.29 (2)	1.35 (2)	1.21 (2)	1.31 (2)	0.01 (2)	0	0
Na(1)	3.8 (2)	2.8 (2)	2.6 (2)	6.2 (6)	−1.7 (3)	0	0
Na(2)	3.4 (2)	3.4 (4)	3.4 (4)	3.4 (4)	−0.1 (3)	−0.3 (3)	0.4 (3)
Na(3)	4.6 (5)	6.1 (11)	5.4 (10)	2.5 (7)	0	0	0
Na(4)	2.0 (2)	1.9 (4)	2.0 (5)	2.1 (4)	0.7 (4)	1.0 (4)	−0.0 (3)
Si(1)	1.38 (4)	1.44 (10)	1.45 (10)	1.24 (10)	0.46 (14)	0	0
Si(2)	1.47 (4)	1.26 (8)	1.18 (7)	1.97 (9)	−0.03 (7)	0.04 (8)	−0.04 (6)
Si(3)	1.32 (5)	1.34 (11)	1.39 (11)	1.22 (13)	0.20 (10)	0	0
Si(4)	1.34 (4)	1.33 (8)	1.14 (9)	1.56 (10)	−0.03 (7)	−0.16 (7)	0.06 (7)
O(1)	2.92 (13)	2.4 (2)	3.2 (2)	3.2 (3)	0.7 (3)	1.0 (3)	−0.2 (2)
O(2)	1.95 (10)	2.3 (2)	1.8 (2)	1.8 (2)	−0.4 (2)	0.2 (2)	0.5 (2)
O(3)	2.0 (2)	2.3 (4)	1.5 (3)	2.3 (4)	0.4 (3)	0	0
O(4)	1.9 (2)	1.3 (3)	2.0 (3)	2.4 (4)	−0.2 (3)	0	0
O(5)	1.9 (2)	2.1 (4)	1.4 (4)	2.3 (5)	0	0	0.6 (3)
O(6)	2.2 (2)	3.6 (4)	1.1 (3)	1.9 (4)	−0.0 (3)	0	0
O(7)	2.2 (2)	2.5 (4)	2.3 (4)	1.7 (4)	0.0 (3)	0	0
O(8)	2.02 (11)	1.9 (2)	1.9 (2)	2.3 (3)	−0.2 (2)	−0.6 (2)	0.2 (2)
O(9)	2.53 (12)	1.7 (2)	2.3 (2)	3.6 (3)	−1.1 (3)	−0.6 (2)	−0.2 (2)
O(10)	1.9 (2)	3.0 (4)	1.7 (3)	1.2 (4)	0.4 (3)	0	0
O(11)	2.2 (2)	2.9 (4)	1.6 (3)	2.1 (4)	0	0.1 (3)	0
$O_w(1)$	8.5 (5)	17 (2)	5.3 (7)	3.8 (7)	0.8 (6)	0	0
$O_w(2)$	5.3 (4)	4.5 (8)	8.9 (12)	2.6 (6)	1.1 (8)	1.4 (7)	2.9 (8)

fractional occupancies and chemical species residing in these additional sites were determined on the basis of bond distances, charge balance and refinement of the site occupancies themselves, as discussed below. The final value of the weighted residual, $wR(F^2)$, using anisotropic thermal parameters for all atoms (including water molecules and Na atoms in partially occupied sites) was 8.09%. The final value of $wR(F)$ was 2.63%. The differences between the earlier structure of Karpov, Pushcharovskii, Pobedimskaya, Burshtein & Belov

Table 5. *Interatomic distances (Å) and bond angles (°) in the neodymium and silicon coordination polyhedra in $Na_3NdSi_6O_{15}.2H_2O$ [numbers in parentheses indicate e.s.d.'s in the last digit(s)]*

Central atom	Bond distance (Å)		Oxygen separation along edge (Å)		O—*M*—O angle (°)
Nd	O(10)	2.301 (7)	O(10)—O(9) 2×	3.166 (8)	85.9 (2)
	O(9) 2×	2.344 (6)	O(10)—O(2) 2×	3.107 (8)	82.6 (2)
	O(2) 2×	2.408 (5)	O(9)—O(9)	3.693 (11)	104.0 (3)
	O(6)	2.530 (7)	O(9)—O(2) 2×	3.039 (7)	79.5 (2)
	O(3)	2.726 (9)	O(9)—O(6) 2×	3.132 (9)	79.9 (2)
			O(2)—O(2)	3.543 (10)	94.7 (3)
	Average	2.44 (14)	O(2)—O(3) 2×	3.106 (9)	74.2 (2)
			O(6)—O(3)	2.553 (10)	58.0 (2)
Si(1)	$O(10)_{term}$	1.579 (8)	O(10)—O(8) 2×	2.625 (8)	110.2 (3)
	$O(8)_{br}$ 2×	1.622 (5)	O(10)—O(3)	2.743 (12)	116.2 (4)
	$O(3)_{br}$	1.651 (8)	O(8)—O(8)	2.632 (11)	108.5 (4)
			O(8)—O(3) 2×	2.609 (8)	105.7 (3)
Si(2)	$O(9)_{term}$	1.578 (6)	O(9)—O(1)	2.701 (10)	115.7 (3)
	$O(1)_{br}$	1.614 (7)	O(9)—O(4)	2.681 (8)	113.7 (4)
	$O(4)_{br}$	1.625 (3)	O(9)—O(5)	2.605 (6)	108.0 (4)
	$O(5)_{br}$	1.641 (4)	O(1)—O(4)	2.526 (6)	102.5 (4)
			O(1)—O(5)	2.632 (10)	108.0 (3)
			O(4)—O(5)	2.655 (7)	108.8 (3)
Si(3)	$O(6)_{term}$	1.589 (9)	O(6)—O(1) 2×	2.662 (11)	112.4 (3)
	$O(1)_{br}$ 2×	1.614 (6)	O(6)—O(3)	2.553 (10)	104.0 (4)
	$O(3)_{br}$	1.650 (7)	O(1)—O(1)	2.626 (11)	108.9 (5)
			O(1)—O(3) 2×	2.667 (8)	109.6 (3)
Si(4)	$O(2)_{term}$	1.575 (6)	O(2)—O(7)	2.653 (8)	112.4 (4)
	$O(7)_{br}$	1.618 (3)	O(2)—O(8)	2.696 (8)	114.5 (3)
	$O(8)_{br}$	1.630 (6)	O(2)—O(11)	2.622 (6)	109.7 (4)
	$O(11)_{br}$	1.631 (4)	O(7)—O(8)	2.552 (6)	103.6 (4)
			O(7)—O(11)	2.632 (9)	108.2 (4)
			O(8)—O(11)	2.642 (9)	108.2 (4)
Averages	$Si—O_{term}$	$Si—O_{br}$	O—O separation	O—Si—O angle	
	1.580 (8)	1.628 (13)	2.64 (5)	109 (4)	

(1977) and that proposed here are also discussed in detail below.

The asymmetric unit of the structure contains 22 atomic sites: 1 Nd, 4 Na (three of which are only partially occupied), 4 Si, 11 O and 2 water (one of which is only half occupied). The atomic coordinates and thermal parameters are listed in Tables 3 and 4, respectively. Those atoms not identified in the earlier model by Karpov, Pushcharovskii, Pobedimskaya, Burshtein & Belov (1977) are listed in bold typeface. Water molecules are designated O_w. It should be emphasized that the floating point origin method of Flack (1983) utilized in this work involves constrained refinement of the z coordinates of all atoms.*

Bond distances, oxygen–oxygen separations and oxygen–cation–oxygen bond angles in the Si and Nd polyhedra are given in Table 5. O atoms bonded to two Si atoms are designated 'bridging' (br), whereas 'terminating' (term) indicates those bonded to only one. Oxygen–cation bond distances for the Na polyhedra are given in Table 6. In the case of Na(2), in addition to the bond distances from the refined coordinates of one of two neighboring Na sites, the distances from what is considered to be the center of a nine-membered cage in which these two sites are located are also listed. The nature of this cage is discussed in greater detail below. Silicon–oxygen–silicon and silicon–oxygen–neodymium angles are provided in Table 7.

Table 6. *Interatomic distances (Å) in the sodium coordination polyhedra in $Na_3NdSi_6O_{15}.2H_2O$ [numbers in parentheses indicate e.s.d.'s in the last digit(s)]*

Na polyhedra

Na(1) distance					
O(9) 2×	2.395 (7)	$O_w(1)$	2.623 (15)	O(7)	3.225 (13)
O(2) 2×	2.445 (7)	$O_w(2)$ 2×	2.70 (2)	O(4)	3.369 (12)
Na(2) distances					
Na′(2)	0.895 (15)	O(5)	2.454 (13)	O(1)	3.080 (12)
$O_w(1)$	2.227 (12)	O′(6)	2.552 (10)	$O_w'(1)$	3.081 (13)
O(6)	2.420 (9)	O(9)	2.916 (10)	Na″(2)	3.227 (15)
From ideal center of nine-membered cage at (4*c*)..2 (1/4, 1/4, 0.1388)					
O(5)	2.413	$O_w(1)$ 2×	2.651	O(1) 2×	3.207
O(6) 2×	2.446	O(9) 2×	3.204		
Na(3) distances					
Na(4) 4×	2.259 (10)	O(10) 2×	2.894 (9)	O(11) 2×	3.058 (15)
Na(4) distances					
$O_w(2)$	1.32 (2)	$O_w'(2)$	2.40 (2)	O(8)	2.607 (11)
Na(3)	2.259 (10)	O(2)	2.525 (10)	O(11)	3.002 (13)
Na(4)	2.30 (2)	O(10)	2.545 (10)	$O_w''(2)$	3.04 (2)

* A list of structure factors has been deposited with the IUCr (Reference: DU0411). Copies may be obtained through The Managing Editor, International Union of Crystallography, 5 Abbey Square, Chester CH1 2HU, England.

Table 7. *Silicon–oxygen–silicon and neodymium–oxygen–silicon angles [numbers in parentheses indicate e.s.d.'s in the last digit(s)]*

Bridging oxygen bond angles (°)

Si—O—Si					
Si(3)—O(1)—Si(2) 2×	151.8 (5)	Si(2)—O(5)—Si(2)	135.1 (6)	Si(2)—O(4)—Si(2)	142.6 (6)
Si(3)—O(3)—Si(1)	141.2 (6)	Si(4)—O(7)—Si(4)	145.6 (6)	Si(4)—O(11)—Si(4)	140.4 (6)
Si(4)—O(8)—Si(1) 2×	136.7 (4)	Average	142 (6)		
Nd—O—Si					
Si(4)—O(2)—Nd	139.6 (3)	Si(3)—O(3)—Nd	94.3 (4)	Si(1)—O(10)—Nd	153.5 (4)
Si(1)—O(3)—Nd	124.5 (4)	Si(2)—O(9)—Nd	139.0 (3)	Si(3)—O(6)—Nd	103.7 (3)

3. Discussion of structure

3.1. *Silica–neodymia framework*

The structure of $Na_3NdSi_6O_{15}.2H_2O$ is shown in Fig. 1. It is based on 'ideal' $(Si_6O_{15})_\infty$ silica layers in which each SiO_4 tetrahedron shares three of its oxygen ions with another tetrahedron, whereas the fourth oxygen ion is unshared. Overall, the layers are parallel to (001), but they are markedly corrugated in {011}, Fig. 2(*a*). They are arranged in a single-layer stacking sequence through repetition by **c**. Fig. 2(*b*), a projection of a single layer along **c**, shows the Si_6O_{15} sheets to contain four-, five-, six- and eight-membered rings. The SiO_4 tetrahedra that form these layers are rather well behaved. The average Si—O_{br} bond length is 1.628 (13) Å and the average Si—O_{term} is 1.580 (8) Å. Both values lie in the range normally observed in phyllosilicates (Liebau, 1987). The average O—O separations, and the average O—Si—O bond angles, are also rather typical: 2.64 (5) Å and 109 (4)°, respectively.

The Nd polyhedra in $Na_3NdSi_6O_{15}.2H_2O$ are defined by seven oxygen ions, as shown in Fig. 3. Seven-fold coordination is rather common for neodymium and the average Nd—O bond length, 2.44 (14) Å, is also quite typical; the shape of the polyhedron is, however, rather unusual and merits some discussion. It can be described as five of the six vertices of an octahedron [O(9)—O(9)—O(2)—O(2) and an apical O(10)] plus a sixth vertex that is 'split' into the O(3) and O(6) locations. The apical Nd—O(10) bond is the shortest in the polyhedron, while the distances to the 'split' vertices are, by far, the longest. The cation is displaced above the plane of the square configuration formed by O(2)

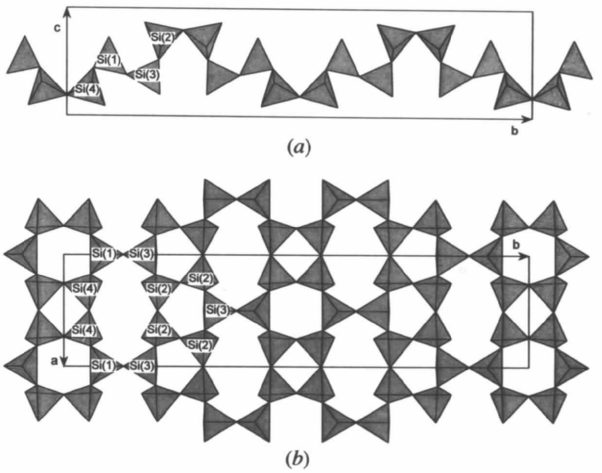

Fig. 2. A single Si_2O_5 layer in $Na_3NdSi_6O_{15}.2H_2O$ (*a*) projected along **a** and (*b*) projected along **c**. Silicon-ion *z* coordinates in (*b*) are: Si(1), 0.5077 (6); Si(2), 0.7117 (3); Si(3), 0.4044 (4); Si(4), 0.2481 (3).

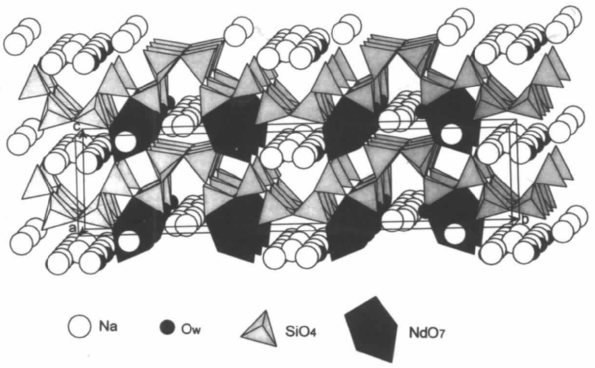

Fig. 1. Structure of $Na_3NdSi_6O_{15}.2H_2O$ viewed along **a**. The SiO_4 and NdO_7 units are represented as polyhedra.

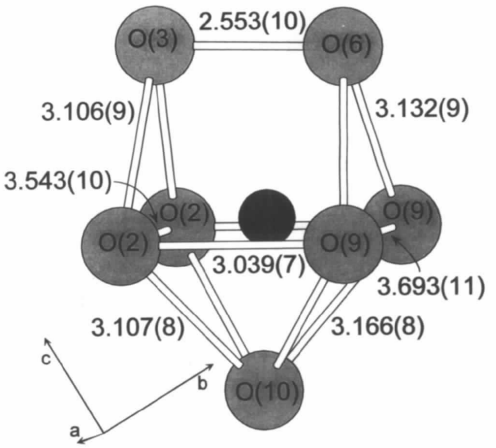

Fig. 3. An isolated NdO_7 polyhedron viewed along **a**. Oxygen–oxygen distances (Å) are shown.

and O(9) and in the direction of the O(3)—O(6) edge. Polyhedra with very similar geometry are commonly found for Bi (and sometimes Pb) in sulfides, although, to be sure, the nature of the bonding in the latter structures is very different and involves a lone electron pair (Armbruster & Hummel, 1987; Kupcík, 1972).

All the terminating O atoms in the silicate tetrahedra participate in forming Nd polyhedra and account for six of the latter's seven vertices. Accordingly, the Nd polyhedra link the Si_2O_5 layers, predominantly by corner sharing, into a rather open, three-dimensional network, Figs. 1 and 4. Specifically, six of the 13 edges (of each Nd polyhedron) link corners of silica tetrahedra between layers immediately above and immediately below the Nd polyhedra. One such set of interlayer O—O bonds is highlighted in Fig. 4(*a*).

The Nd polyhedral edges that span terminal oxygen anions on the SiO_4 tetrahedra create very regular rings, comparable to those in networks that are built entirely of tetrahedral linkages. In Fig. 4(*b*), for example, a six-membered ring can be observed that is built of two pairs of tetrahedra [Si(2)—Si(2) and Si(4)—Si(4)] which are joined by the edges of two Nd polyhedra. The two crystallographically independent Nd—O—Si bond angles in the ring are 139 and 140°, values typical of Si—O—Si angles. In accordance with the role of the neodymium in connecting neighboring Si_2O_5 layers, the Si(2) pair of tetrahedra are in a layer that lies below the Nd atom, whereas the Si(4) pair are in the layer above.

One of the seven Nd vertices, O(3), is a bridging O atom and hence the NdO_7 polyhedron shares one of its edges with an SiO_4 tetrahedron, Fig. 4(*a*). This turns out to be the O(6)—O(3) edge of the Si(3) tetrahedron. Two implications follow from this feature: the shared polyhedral edge should be shortened and the bridging oxygen ion would appear to be highly over-bonded, the sum of the Pauling bond strengths being 17/7. Regarding the first, the O(6)—O(3) edge, with a length of 2.553 (10) Å, is indeed the shortest oxygen–oxygen distance in the structure involving a terminating oxygen ion. Regarding the second, an increase of the bond distances between O(3) and its cation neighbors would reduce the strengths of those bonds and eliminate the apparent oversaturation. It may be noted from Table 5 that the Nd—O(3) bond distance of 2.726 (9) Å is indeed the longest in the polyhedron, being ~0.2 Å larger than the second longest. Similarly, the Si(3)—O(3) distance of 1.650 (7) Å is the longest in any Si tetrahedron; Si(1)—O(3) is the second longest. A complete discussion of the balance of local valence sums, using the relationship between bond strength and experimental interatomic distances developed by Brown & Altermatt (1985), is provided below as part of a comparison of the structural model of the present work with that of Karpov, Pushcharovskii, Pobedimskaya, Burshtein & Belov (1977).

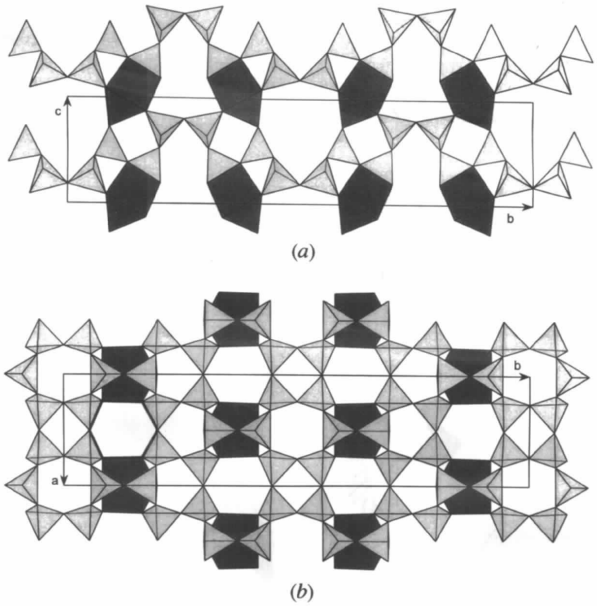

Fig. 4. Silica and neodymia polyhedra in $Na_3NdSi_6O_{15}.2H_2O$; (*a*) structure projected along **a** and (*b*) projected along **c**. See text for discussion of highlighted polyhedral edges.

3.2. *Interstitial species: sodium and water*

The negative charge of the open anionic framework built by Si and Nd polyhedra is balanced by sodium cations lodged in its interstices. The ample size of the cavities, and the hydrothermal conditions under which the phase was synthesized, result in the presence of water molecules in the structure as well. Fig. 5 reveals that three independent channels exist in the structure that provide likely sites for these species. A first extends along [001] at ~1/2, 0.1, *z*. Two additional channels exist along [100] at ~*x*, 1/4, 1/8 and ~*x*, 1/2, 0.8. The sodium ion Na(1) resides in the first channel at 1/2, 0.1240 (2), 0.9743 (15), Fig. 5. This location is at the center of the six-membered ring formed by the Nd, Si(2) and Si(4) polyhedra described previously. The Na(1) atom was present in the structure reported by Karpov, Pushcharovskii, Pobedimskaya, Burshtein & Belov (1977) and was well behaved in the initial stages of our refinement of their model. As indicated in Table 6, it is coordinated by four oxygen nearest-neighbors and by both water molecules later introduced into the structure. Two additional oxygen neighbors are located at somewhat further distances.

A second sodium ion, Na(2), was placed at a site of residual density in the smaller of the two [100] channels. The position is coordinated by seven oxygen ions and two water molecules eventually introduced into the structure, Fig. 5(*a*). Attempts to refine the structure with Na(2) situated at the center of the polyhedron defined by these nine atoms led to unreasonably large and anisotropic thermal parameters, suggesting that the polyhedron is too large for Na. Indeed, the distances

from the central position at 1/4, 1/4, 0.1388 average 2.8 (4) Å [or 2.9 (4) Å when only the seven oxygen neighbors are considered]. Accordingly, the Na(2) cation was placed at two sites on either side of this cage, each with 1/2 occupancy. There, the cation is coordinated by four nearest neighbors at distances less than 2.6 Å, and another three at distances between 2.9 and 3.1 Å.

The second of the two [100] channels (at $\sim x$, 1/2, 0.8) is extraordinarily large, Fig. 5(*a*), with a cross section of 5.56 × 7.12 Å along **b** and **c**, respectively (as measured from the centers of the surrounding anions). Within this expanse, two significant density maxima were found in difference maps and identified as partially occupied sodium-ion sites, Na(3) and Na(4). Starting with equal temperature factors for both sites, the thermal parameters, coordinates and site occupancies were refined for these atoms. The occupancies were constrained such that the multiplicities of the sites (two and eight, respectively) times their respective occupancies provided the remaining four sodium ions per cell. Refinement of the positions proceeded smoothly to convergence. All correlation coefficients between parameters related to Na(3) and Na(4) remained less than 0.5.

One of the two water molecules in the structure, $O_w(2)$, was placed at a location of residual electron density in the same [100] channel as that containing Na(3) and Na(4). Highly anisotropic thermal vibration was displayed by the atom placed in this site. Therefore, in the final stages of refinement it was split into two half-occupied positions, which settled on a separation of only 1.13 (3) Å. A second water molecule, $O_w(1)$, was also assigned to a site that was revealed, in the difference maps, to also display residual electron density. This feature was noted, as well, by Karpov, Pushcharovskii, Pobedimskaya, Burshtein & Belov (1977), but no atom was assigned to this location in their model. Refinement of positional and thermal parameters for $O_w(1)$ also yielded very anisotropic temperature factor coefficients. Splitting of this atom into two locations, as carried out with $O_w(2)$, however, neither improved the residual nor lowered any standard deviation. The large thermal parameters found for both water molecules could possibly reflect site occupancies that are somewhat lower than those that were assigned to provide a cell content of eight H_2O in the final refinement. The thermogravimetric analysis suggests that indeed fewer than two water molecules may be present per formula unit, but there was no convenient experimental method for determining the water content of the specific crystal used in the X-ray analysis.

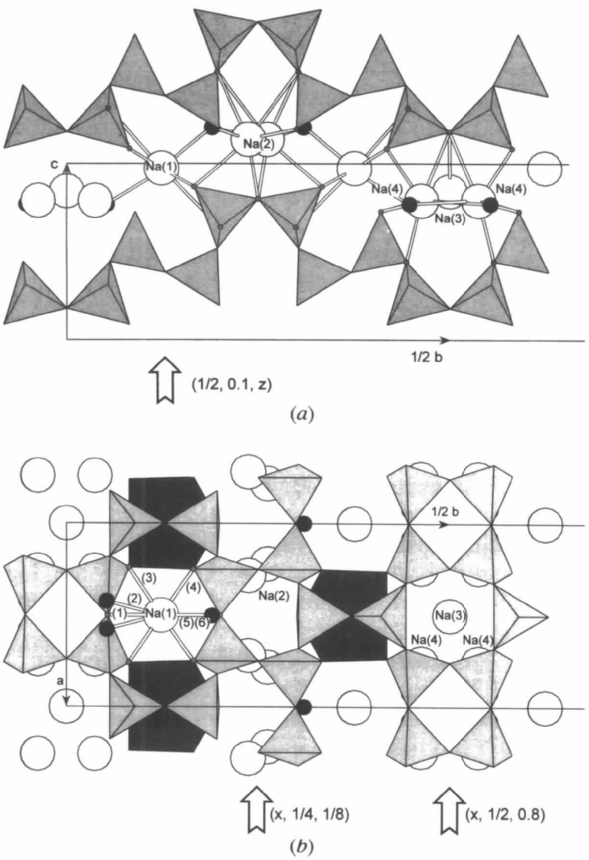

Fig. 5. Expanded view of the structure of $Na_3NdSi_6O_{15}.2H_2O$ showing sodium-ion locations, bonding geometry and channels, the location and direction of the latter indicated with large arrows; (*a*) projection along **a** and (*b*) projection along **c**. Na(1) elevation in (*b*) is 0.9743 (15) and bonds are (i) to O(7) at elevation 1.3124 (12), (ii) to $O_w(2)$ at elevation 0.769 (2), (iii) to O(2) at elevation 1.0851 (8), (iv) to O(9) at elevation 0.8680 (9), (v) to $O_w(1)$ at elevation 1.206 (2) and (vi) to O(4) at elevation 0.6374 (12) Å. Bond distances are given in Table 6.

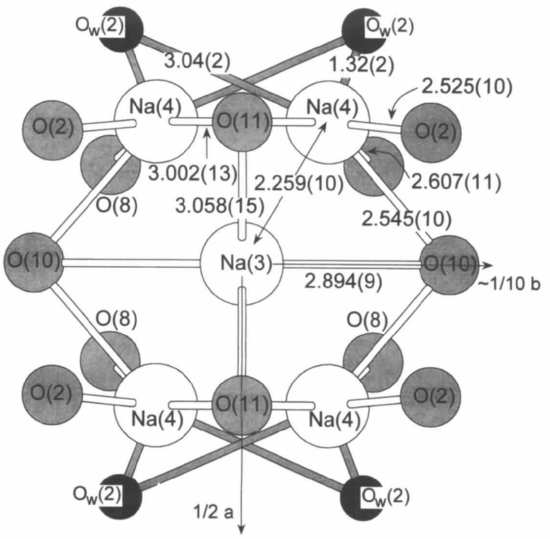

Fig. 6. Bonding geometry about Na(3) and Na(4) sites in a projection along **c**. Sodium–oxygen and sodium–water distances (Å) are provided.

Like the neodymium polyhedra, the sodium polyhedra serve to link neighboring silicate layers, Fig. 5. The Na(1) ion is coordinated by two O(9) anions from a layer beneath it and two O(2) anions from a layer above. If the two half-occupied $O_w(2)$ sites are considered as a single water molecule and the bond to $O_w(1)$ is included, the coordination about Na(1) is octahedral, Fig. 5(*b*). Na(2) is disordered over two closely spaced sites within a nine-cornered cage, Fig. 5(*a*), which, again, involves oxygen ions from two different Si_2O_5 layers. The bonding geometry about the Na(3) and Na(4) sites is shown in Fig. 6. The Na(3) ion is located rather centrally within the larger of the two [100] channels and, as a consequence, is quite distant from any surrounding anions. The nearest oxygen neighbors are two O(10) atoms at 2.894 (9) Å and two O(11) atoms at 3.058 (15) Å, configured to form a distorted tetrahedron about Na(3). The two O(10) atoms are located in the silicate layer below Na(3), whereas the two O(11) atoms are in the layer above. The low coordination and large bond distances about Na(3) suggest that this is not an interstitial position of low energy. The sodium ions can instead tuck themselves into the Na(4) site only 2.259 (10) Å away. Like the Na(3) site, this position is coordinated by four oxygen ions, but may be energetically preferable as the neighbors occur at closer locations. It is relevant to note that the nearest neighbor site to Na(4) is $O_w(2)$. Its close proximity, only 1.32 (2) Å from the cation position, precludes the simultaneous occupancy of neighboring Na(4) and $O_w(2)$ sites. As the average occupancy of $O_w(2)$ is 0.5 and that of Na(4) 0.365 (7), simultaneous occupation can easily be avoided.

3.3. *Comparison with the structural model of Karpov, Pushcharovskii, Pobedimskaya, Burshtein & Belov (1977)*

The lattice constants reported by Karpov, Pushcharovskii, Pobedimskaya, Burshtein & Belov (1977), a = 7.387 (2), b = 30.87 (1), c = 7.120 (3) Å, for a phase believed to have the composition $NaNdSi_6O_{13}(OH)_2.nH_2O$, are very close to the values 7.385 (2), 30.831 (7) and 7.1168 (13) Å, respectively, obtained for the phase examined in the present study. Similarly, the coordinates obtained for all the Si, Nd and O framework atoms, Table 3, are in good agreement. The small differences would appear to arise only from the higher precision of the present study [$wR(F)$ = 2.63% in contrast to the result $R(F)$ = 8.9% of Karpov, Pushcharovskii, Pobedimskaya, Burshtein & Belov (1977)]. It therefore seems virtually certain that the present work and that of Karpov, Pushcharovskii, Pobedimskaya, Burshtein & Belov (1977) have studied one and the same phase. The different compositions deduced, $Na_3NdSi_6O_{15}.2H_2O$ and $NaNdSi_6O_{13}(OH)_2.nH_2O$, result from different and, we believe, incorrect crystal-chemical assumptions that were made in the earlier model regarding the manner in which charge compensation with the neodymia–silica framework is achieved.

The density of 2.75 g cm^{-3} measured by Karpov, Pushcharovskii, Pobedimskaya, Burshtein & Belov (1977) is in much better agreement with the calculated value of 2.68 g cm^{-3} for the composition $Nd_3NdSi_6O_{15}.2H_2O$, deduced in the present work. In contrast, a composition of $NaNdSi_6O_{13}(OH)_2.nH_2O$ provides, for $n \simeq 2$, a calculated density of 2.52 g cm^{-3}. The experimental chemical analysis performed by Karpov, Pushcharovskii, Pobedimskaya, Burshtein & Belov (1977) revealed the ratio of the weight percentages of SiO_2 to Na_2O to be 0.25. This is in far better agreement with the composition that we have proposed, for which SiO_2:Na_2O = 0.28, than with $NaNdSi_6O_{13}(OH)_2.nH_2O$, for which SiO_2:Na_2O = 0.09.

In addition to better fitting the macroscopic chemical and physical data, our model is more realistic from a crystal-chemical viewpoint. In the present model charge compensation of the negative silica–neodymia framework is achieved entirely by Na ions, whereas the model of Karpov, Pushcharovskii, Pobedimskaya, Burshtein & Belov (1977), containing only one Na atom per formula unit, assumes the remainder of the positive charge required for overall neutrality to come from hydrogen ions (protons) in the form of hydroxyl groups distributed over the four terminating oxygen positions: O(2), O(6), O(9) and O(10). The longest Si—O_{term} bond distance observed by Karpov, Pushcharovskii, Pobedimskaya, Burshtein & Belov (1977) in $NaNdSi_6O_{13}(OH)_2.nH_2O$ was 1.606 Å, a value which is rather high, but not large enough to correspond to a Si—OH bond distance; a value of 1.685 Å has been determined in $K_3NdSi_3O_8(OH)_2$, for example [Hale (*sic*), Maier, Wuensch & Laudise, 1993]. Accordingly, Karpov, Pushcharovskii, Pobedimskaya, Burshtein & Belov (1977) were correct in selecting a distributed rather than isolated position for the OH group. However, it seems unlikely that their bond lengths [$\langle d(\text{Si—O}_{term})\rangle$ = 1.58 (2) Å] are long enough to support the presence of even a distributed proton. A second structural anomaly in the model of Karpov, Pushcharovskii, Pobedimskaya, Burshtein & Belov (1977) lies in the coordination geometry about Na(1). Without the introduction of interstitial water molecules, this sodium site is coordinated by four O atoms [2 × O(2) and 2 × O(9)], in an almost perfect square-planar configuration, Fig. 5, an environment which is quite unlikely for sodium. As stated earlier, the presence of water molecules in the present model leads to essentially octahedral coordination.

A quantitative assessment of the impact of the three Na ions on local charge neutrality (and, therefore, the correctness of the present model) can be made in terms of valence sums. In Table 8 we provide the sum of the bond strengths (or valences) at each atomic site, according to the relationship between bond strength

Table 8. *Bond strengths and summation of bond strengths for ions in* $Na_3NdSi_6O_{15}.2H_2O$

Bond strengths calculated according to $s = \exp[(r_o - r)/0.37]$, where r_o is 2.105 (5) for $Nd^{3+}—O^{2-}$, 1.624 (1) for $Si^{4+}—O^{2-}$ and 1.803 (3) for $Na^+—O^{2-}$ (Brown & Altermatt, 1985). The notation × no. indicates the multiplicity of the bond, *C* indicating the cation has multiple such bonds and *A* that the anion has multiple bonds. Oxygen ions listed in bold typeface indicate that the anion is a terminating species. $\sum(1)$ corresponds to the sum of the bond strength at the anion sites excluding Na(2)–Na(4), whereas $\sum(2)$ is the sum indicating all cations. For partially occupied sites, the bond strength provided refers to a fully occupied site; partial occupancies are accounted by summing only the appropriate fraction of the value of the bond strength. $\sum$ corresponds to the summation of the bond strength at the cation sites. The contribution of water molecules has been ignored as the orientation of these molecules is unknown.

Anion	Nd	Si(1)	Si(2)	Si(3)	Si(4)	Na(1)	$\sum(1)$	Na(2) 1/2 occupancy	Na(3) 0.54 occupancy	Na(4) 0.37 occupancy	$\sum(2)$
O(1)			1.03	1.03×2*C*			2.06	0.03			2.08
O(2)	0.44×2*C*				1.14	0.17×2*C*	1.75			0.14	1.80
O(3)	0.19	0.94		0.93			2.06				2.06
O(4)			1.00×2*A*			0.02	2.02				2.02
O(5)			0.96×2*A*				1.92	0.18×2*A*			2.10
O(6)	0.32			1.09			1.41	0.19×2*A*			1.73
								0.13×2*A*			
O(7)					1.01×2*A*	0.02	2.04				2.04
O(8)		1.01×2*C*			0.98		1.99			0.11	2.03
O(9)	0.52×2*C*		1.14			0.21×2*C*	1.87	0.05			1.90
O(10)	0.59	1.12					1.71		0.05×2*C*	0.14×2*A*	1.84
O(11)					0.98×2*A*		1.96		0.03×2*C*	0.04×2*A*	2.01
$\sum$	3.02	4.08	4.13	4.08	4.11	0.80		0.58	0.16	0.43	

and experimental interatomic distances developed by Brown. The values obtained both with (present model) and without [Karpov, Pushcharovskii, Pobedimskaya, Burshtein & Belov (1977) model] the Na(2)–Na(4) ions are compared. Partial occupancies in the present structural model have been accounted for. The data show that the inclusion of the three additional sites identified as interstitial Na positions results in summations of bond strengths that more closely match the charge of the oxygen ions than in their absence. In particular, O(6), part of the shared SiO_4–NdO_7 edge, has a disturbingly low valence sum of only 1.41 when only silicon, neodymium and Na(1) cations are considered. When contributions from all four sodium sites are included, the valence sum rises to a more satisfactory 1.73, a value only slightly less than that obtained for the three other terminating oxygen ions.

Finally, it is important to note that Karpov, Pushcharovskii, Pobedimskaya, Burshtein & Belov (1977) reported residual electron density at three of the five additional interstitial sites identified in the present work. The coincidence of these sites renders it unlikely that Karpov, Pushcharovskii, Pobedimskaya, Burshtein & Belov (1977) examined a similar, but fundamentally distinct, compound to that described here.

3.4. *Pathways for ion transport*

As Nd, Si and O all form integral parts of the structural framework of $Na_3NdSi_6O_{15}.2H_2O$, ionic conduction in this compound would presumably occur by the transport of sodium ions. As a prerequisite for fast-ion transport, the sodium ions must reside in pathways that connect energetically equivalent sites, present in numbers greater than the number of sodium ions available to fill them. These sites should, ideally, be connected *via* face-shared polyhedra, in order that the barrier to migration between sites be low. A low migration barrier is further suggested when the charge carrier exhibits large thermal vibrations, particularly along the direction of the jump between sites.

Any of the three crystallographically independent channels could, in principle, serve as pathways for ion migration. The channel along [001], Fig. 5(*b*), appears particularly conducive to sodium-ion transport as it is spacious, yet, relatively empty, containing only the Na(1) ion. This sodium ion is situated at a bottleneck position within the channel that just accommodates its bonding requirements, indicating that the Na(1) location is determined primarily by coulombic rather than steric considerations. This, together with the large thermal vibration parameter of Na(1) in the *z* direction, $U_{33} = 6.2 \times 10^{-2}$ Å^{-2}, suggests that the Na(1) site corresponds to a shallow local energy minimum. The distance between normal sites (along this channel) is a rather long 7.117 (1) Å and the polyhedra about the neighboring sites share no ions. Therefore, it is quite likely that interstitial sites exist between normal sites and that these will aid in the transport of sodium *via* this rather spacious channel. In sum, it is reasonable to expect high Na(1) mobility along *z*.

The second sodium ion is located within the smaller of the two channels that extend along *x*. The half-occupied Na(2) sites within the nine-membered cage are separated by only 0.895 (15) Å. The proximity implies that simultaneous occupation of two sites within one cage is unlikely and, hence, unoccupied Na(2) sites cannot serve

as interstitial positions for migrating ions. If, however, vacancies can be generated along these channels by the displacement of Na ions into other interstitial sites in the structure, the likelihood of transport is quite high.

The prospect of ion transport along the larger of the two [100] channels, Fig. 5, is also quite good. The Na(3)–Na(4) sites within it form a virtually continuous path along x. The stoichiometry of $Na_3NdSi_6O_{15}.2H_2O$ requires that of every five sites within the channel, on average, only two will be (fully) occupied. The sites are distant enough from one another, however, that any particular group of five sites, such as depicted in Fig. 6, could, at least temporarily, accommodate more than two sodium ions. The Na(3)—Na(4) distance is 2.259 (10) Å, for example, whereas the Na(4)—Na(4) distances are 2.30 (2) and 3.57 (2) Å. This channel, then, meets the structural requirement that the number of energetically equivalent sites exceed the number of ions available to occupy them. The only significant barrier to sodium ion migration arises from the $O_w(2)$ water molecules, but these would probably not constitute a serious impediment as they occupy only 50% of their sites. In addition to the intrinsically high degree of disorder within the channel, the large thermal vibrations of Na(3), which are, in fact, greatest along the proposed jump direction (U_{11} = 6.1 × 10^{-2} Å^2), further support the notion of fast-ion transport *via* this third pathway.

Other, less direct, pathways for sodium-ion migration also exist in the neodymia–silica framework of $Na_3NdSi_6O_{15}.2H_2O$. For example, transport along the z direction might take place *via* Na(3)→Na(3) jumps through the six-membered SiO_4 rings consisting of four Si(4) tetrahedra and two Si(1) tetrahedra, Fig. 5(*b*). The site-to-site distance is 7.117 (1) Å and the shortest oxygen–oxygen distance across the ring is 3.80 (2) Å, a rather tight squeeze for sodium-ion passage, but transport is conceivable assuming some structural relaxation takes place. Furthermore, the low occupancy of the Na(3) sites favors transport *via* this path. The outlook for high ionic conductivity along the y direction is not as favorable as that for the two directions already discussed. The corrugation of the layers requires that any migration along the y direction follows a 'zigzag' path that conforms to the contours of the silica layer and, in addition, circumvents the Nd polyhedra.

To date we have been unable to grow crystals of $Na_3NdSi_6O_{15}.2H_2O$ of a size large enough to allow conductivity measurements. Attempts to densify pressed pellets were not made as it was expected such steps would lead to melting and the formation of a stable glass. It is hoped that efforts to synthesize larger crystals will be successful and will then enable an examination of the transport properties and their dependence on crystallographic direction, as was carried out for phases encountered in the K_2O–Nd_2O_3–SiO_2 system [Haile, Wuensch, Siegrist & Laudise, 1992; Hale (*sic*), Maier, Wuensch & Laudise, 1993].

4. Concluding remarks

We have described the structure of $Na_3NdSi_6O_{15}.2H_2O$, an 'ideal' layer silicate, and believe it to be the correct formulation of a structure previously reported for $NaNdSi_6O_{13}(OH)_2.nH_2O$. The present work not only found residual density at exactly the coordinates reported by Karpov, Pushcharovskii, Pobedimskaya, Burshtein & Belov (1977), but assigns Na to one and water molecules to the remaining pair of sites. This assignment of Na cations to interstitial sites in the present work successfully provides charge balance for the framework oxygen ions and also results in acceptable interatomic distances. We have also concluded that, based on the existence of channels within the structure of $Na_3NdSi_6O_{15}.2H_2O$, the intrinsic disorder and the large thermal vibration parameters of the Na atoms, that, both along and perpendicular to the layers, this silicate is promising as a fast-ion conductor. Moreover, we expect the conductivity to behave somewhat anisotropically, with the highest conductivity along the [100] direction and the lowest along [010].

We are indebted to Dr Karl Peters of the Max-Planck-Institut für Festkörperforschung for providing single-crystal intensity data and to Dr Peter Höhn for aid with the structure determination. Nubia Carioca, also of MPI, kindly performed TGA experiments and Mike Jercinovic, of the Massachusetts Institute of Technology, supplied the results of microprobe analyses. Figures were drawn using the *ATOMS* program by Shape Software. S. Haile is grateful to the AT&T Cooperative Fellowship Program, the Fulbright Foundation and the Alexander von Humboldt Foundation for providing financial support at various stages of this research.

References

Armbruster, T. & Hummel, W. (1987). *Am. Mineral.* **72**, 821–831.

Brown, I. D. & Altermatt, D. (1985). *Acta Cryst.* B**41**, 244–247.

Cromer, D. T. & Waber, J. T. (1974). *International Tables for X-ray Crystallography*, Vol. IV, Table 2.2A, pp. 128–134. Birmingham: Kynoch Press. (Present distributor Kluwer Academic Publishers, Dordrecht.)

Flack, H. D. (1983). *Acta Cryst.* A**39**, 867–881.

Goodenough, J. B., Hong, H. Y.-P. & Kafalas, J. A. (1976). *Mat. Res. Bull.* **11**, 203–220.

Haile, S. M. (1992). PhD thesis. Massachusetts Institute of Technology, Cambridge, Massachusetts, USA.

Haile, S. M., Wuensch, B. J. & Laudise, R. A. (1993). *J. Cryst. Growth*, **131**, 373–386.

Haile, S. M., Wuensch, B. J., Siegrist, T. & Laudise, R. A. (1992). *Solid State Ion.* **53/56**, 1292–1301.

Hale (*sic*), S. M., Maier, J., Wuensch, B. J. & Laudise, R. A. (1993). In *Proc. NATO Workshop Fast Ion Transport in Solids*, edited by B. Scrosati, pp. 315–326. Amsterdam: Kluwer Academic Publishers.

Karpov, O. G., Pushcharovskii, D. Yu., Pobedimskaya, E. A., Burshtein, I. F. & Belov, N. V. (1977). *Sov. Phys. Dokl.* **22**, 464–466.

Kupcík, V. (1972). In *Handbook of Geochemistry*, edited by H. H. Wedepohl, Vol. II/3, pp. 83A1–83A7. Berlin–Heidelberg: Springer-Verlag.

Laudise, R. A. (1987). In *Advanced Crystal Growth*, edited by P. M. Dryburgh, B. Cockayne & K. G. Barraclough. New York: Prentice Hall.

Liebau, F. (1987). *Structural Chemistry of Silicates: Structure, Bonding, and Classification*. Berlin: Springer-Verlag.

Schamber, F., Wodke, N. & McCarthy, J. (1981). *ZAF Matrix Correction Procedure for Bulk Samples: Operation and Program Description*, 31 pp. Tracor Northern Publication TN-2120, Middleton, Wisconsin, USA.

Sheldrick, G. M. (1993). In *Crystallographic Computing 6*, edited by H. D. Flack, L. Parkanyi & K. Simon, pp. 100–110. New York: Oxford University Press.